

## Experimental Study on Dehumidification Technology using Honeycomb Desiccant Block

Yaningsih, Indri

Department of Energy and Environmental Engineering, Interdisciplinary Graduate School of Engineering Sciences, Kyushu University | Thermal Science and Engineering Division, International Institute of Carbon-Neutral Energy Research (I2CNER), Kyushu University

Mahmood, Muhammad Hamid

Department of Energy and Environmental Engineering, Interdisciplinary Graduate School of Engineering Sciences, Kyushu University

Wijayanta, Agung Tri

Department of Mechanical Engineering, Faculty of Engineering, Sebelas Maret University

Miyazaki, Takahiko

Department of Energy and Environmental Engineering, Interdisciplinary Graduate School of Engineering Sciences, Kyushu University | Thermal Science and Engineering Division, International Institute of Carbon-Neutral Energy Research (I2CNER), Kyushu University

他

<https://doi.org/10.5109/1936212>

---

出版情報 : Evergreen. 5 (2), pp.11-18, 2018-06. 九州大学グリーンアジア国際リーダー教育センター  
バージョン :

権利関係 : Creative Commons Attribution-NonCommercial 4.0 International



# Experimental Study on Dehumidification Technology using Honeycomb Desiccant Block

Indri Yaningsih<sup>1,2</sup>, Muhammad Hamid Mahmood<sup>1</sup>, Agung Tri Wijayanta<sup>3\*</sup>,  
Takahiko Miyazaki<sup>1,2\*</sup>, Shigeru Koyama<sup>1,2</sup>

<sup>1</sup>Department of Energy and Environmental Engineering, Interdisciplinary Graduate School of Engineering Sciences, Kyushu University, Japan

<sup>2</sup>Thermal Science and Engineering Division, International Institute of Carbon-Neutral Energy Research (I<sup>2</sup>CNER), Kyushu University, Japan

<sup>3</sup>Department of Mechanical Engineering, Faculty of Engineering, Sebelas Maret University, Indonesia

\*Author to whom correspondence should be addressed,

\*E-mail: miyazaki.takahiko.735@m.kyushu-u.ac.jp, agungtw@uns.ac.id

(Received December 19, 2017; accepted June 4, 2018).

The current research highlights the potential of using desiccant dehumidification technology with the merits of low initial energy consumptions. The system consists of desiccant (DSC) block units, dehumidification and regeneration air sources, air flow control valves, and a set of the heat exchanger. Attention was given to the DSC blocks. The blocks were made of hydrophilic polymer with honeycomb shaped. The present study focuses on the heat and mass transfer (HMT) characteristics to enhance the performance of the system. Three different process air temperatures of 20°C, 25°C, and 35°C were investigated under constant regeneration air temperature of 55°C and inlet air velocity of 0.1 kg/s. For each process air temperature, four different switching time ratios were also introduced to examine the HMT balance of the DSC blocks. The results revealed that the dehumidification capacity of the DSC system has high potential as air conditioning devices. The discrepancy of HMT found was less than 8%. Hence, the experimental methods were reliable to conduct the further experiments.

Keywords: desiccant, dehumidification, regeneration, heat transfer, mass transfer

## 1. Introduction

Air conditioning to achieve the human thermal comfort is an essential role in human life, especially in humid and hot climates area. Traditional vapor-compression systems are a widely used method to accomplish this condition. However, this system is primarily driven by using refrigerant as working fluids which has high potential on the ozone depletion layer. High-grade energy is also required. A significant amount of energy, that used to achieve this air, is mostly coming from conventional energy resources. Due to some drawbacks of the vapor-compression system, alternative technology should be proposed.

A desiccant dehumidification system (DDS) has been proposed as an alternative technology and practical solution to provide the air conditioning due to the main merits of low initial energy consumption, no required refrigerant, and low-cost air conditioning system. The desiccant (DSC) system could provide the same effect with traditional vapor-compression by controlling the humidity using its own temperature. This technology

also reduces the energy consumption largely by employing of some waste heat from the industrial processes or power plant and utilizing the renewable energy sources. If the DSC system is appropriately applied, it could save more energy than the traditional system.

Nowadays, the development of DSC technology has been paid considerable attention by researchers<sup>1-5)</sup>. Majumdar and Worek<sup>1)</sup> studied desiccant cooling system by using advanced desiccant matrices. The parameters related to indoor and outdoor conditions were numerically studied to evaluate the performance of the system. They proposed a detail mathematical model for calculating the moisture diffusion and heat conduction of the desiccant dehumidifier. They found that regeneration and indoor air temperature and outdoor humidity ratio were significantly affected by the performance of the system. Dhar and Singh<sup>2)</sup> investigated hybrid air-conditioning system using solid desiccant. They investigated the performance of the hybrid air-conditioning system by considering the energy consumption and initial cost. Hybrid air conditioning is

defined as the combination between the vapor compression machine and desiccant system. The results were compared with the conventional system using refrigerated cooling coils. A hybrid air-conditioning system with desiccant-based could achieve high energy saving as compared to the traditional system, especially in hot and dry weather condition. Cui et al.<sup>3)</sup> developed new adsorbent for the desiccant cooling system. The adsorption isotherm of the zeolite 13X, silica gel, DH-5, and D-H7 were also investigated. For cooling cycle, DH-5 and DH-7 were suitable because their ability to provide higher cooling capacity 2.2 and 1.3 times as compared to silica gel and zeolite 13X. Numerical study of desiccant wheel air conditioning was studied by Nia et al.<sup>4)</sup>. They developed the simulation by using MATLAB Simulink to evaluate the performance of adiabatic rotary dehumidifier. The prediction of the temperature and humidity of the outlet air was calculated by using the heat and mass transfer model. The results showed that the simulation and published experimental data were agreed well with the maximum difference of 2%. Stabat and Marchio<sup>5)</sup> numerically studied rotary desiccant dehumidifiers. The model also included the heat and mass transfer inside the desiccant wheel system. They simplified the model by assuming some parameters such as thermal capacity ratio, effectiveness and purge section. Considering the experimental data and manufacture's data, their model offers a better result.

As aforementioned in the literature, study for developing desiccant system was experimentally and numerically studied by modifying essential parameters. The important process of the system was related to the contact between the air and surface of the desiccant material which considered as a variable in many types of air conditioning system research. Fundamental principal work of the DSC system is made up of three steps. First, the DSC is removing the water from the process air. Since the migration of the water vapor occurs, the humidity of the DSC will be increased. Second, to make the system can be repeated the DSC must be regenerated. Thus, the DSC is heated by a different airflow (regeneration air) to remove the water vapor. The DSC should be dried enough to ensure the ability for adsorbing water vapor for next process. After that, the DSC material needs to be cooled to the initial temperature so that the process can be continuous.

Considering the low performance of the DSC system, an effort to enhance the performance of the system becomes necessary at present. For the adsorption/desorption process, the heat and mass transfer (HMT) performance of the adsorbents is a critical factor which is affecting the DSC system process<sup>6)</sup>. In this regard, several studies were performed on HMT analysis through experimental and analytical to upgrade the performance of the DSC system. Majumdar<sup>7)</sup> conducted an HMT investigation by using the composite DSC material pore structure for dehumidification. The composites were

made of the silica gel particles and inert particles. The results show the increase of the capacitance ratio is improving the cooling capacity. Conversely, the cooling capacity tends to decrease with an increase of a fraction of the inert material. Sphaier and Worek<sup>8)</sup> performed the developing of a mathematical model for the transfer process. The transport phenomena inside the porous sorbent bed were described in detail to explain the HMT on the DSC system. It is found that new dimensionless formulation is successfully validated with the previous study including the experimental data. It is also observed that the performance could be improved by reducing the felt thickness. Inaba et al.<sup>9)</sup> proposed the experimental study on the HMT characteristics of the organic sorbent coated on a heat exchanger. They have concluded that the mass transport behavior depends on the mass transfer resistance of the organic sorbent. Furthermore, they have also obtained that the non-dimensional average mass transfer coefficient is a function of Reynolds number and temperature.

Nobrega and Brum<sup>10)</sup> proposed a comparative study of HMT on passive and active DSC wheels. The characteristics of the DSC was developed by using the mathematical model. The results show the different behaviors between two DSC wheels. For the passive dehumidification, the HMT influences the enthalpy recovery while the active dehumidification HMT has an impact on the regeneration temperature and adsorption capacity of the system. Li et al.<sup>11)</sup> investigated the HMT characteristics for a DSC-coated fin-tube heat exchanger during the adsorption and desorption process. They have found that the parameters which affect the mass-transfer coefficient are the air flow rate, the temperature and humidity of the DSC felt. They have developed an average overall mass-transfer coefficient and compared to the experimental values. They have found that the deviation values fall within  $\pm 20\%$ . In characterizing the HMT in polymer DSC wheels, an experimental investigation has been carried out by Kang and Lee<sup>12)</sup>. Three different polymers and wall thicknesses have been tested under various conditions of air velocity and rotation speed to investigate the performance of the system. It is revealed that the higher dehumidification performance is achieved due to the smaller increase of sensible temperature. Based on the review of the previous study, the behavior of the DSC system can be determined by some combined parameters. Most of them are observed the temperature and humidity variations on the performance of the system, intensively in DSC block. However, another crucial operating condition that is called switching time is rarely reported. Switching time is defined as the required time to complete the dehumidification and regeneration process which also determines the performance of the DSC system. Some efforts have been performed with experimental and numerical approaches by modifying the switching time to change the period of the dehumidification and

regeneration time. Chang et al.<sup>13)</sup> investigated the dehumidification effect by using a two-desiccant-coated heat exchanger. It is found that if the switching time is appropriately considered and applied to the system, it could enhance the performance significantly. Sultan et al.<sup>14)</sup> reported that switching time could control the dehumidification capacity of the system, however, it depends on the application of the system. Thus, in this present study, we also consider varying the switching time with the ratio that provides the best performance of the system.

Consequently, from the above literature, the heat and mass transfer analysis have great importance on the performance of the system. Most of the works were provided the equation to predict the HMT behaviors of the DSC system. However, there is no study that validated the HMT balance from the experimental data. From this reason, it becomes our motivation to investigate the HMT balance of DDS by using the honeycomb block. The honeycomb block is made from hydrophilic polymer. Moreover, the present work is conducted under a wide range of temperature of the process air.

## 2. Experimental Facility

### 2.1 Apparatus Setup

The schematic diagram of the DDS is depicted in Fig. 1.

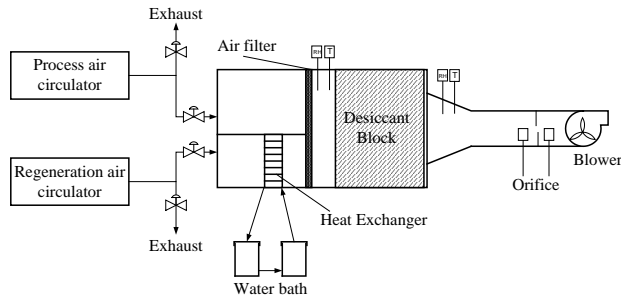


**Figure 1.** Schematic diagram of the DDS.

The DDS is an open-cycle unit, which is placed in the temperature and relative humidity room conditioned. The system consists of DSC block units, dehumidification and regeneration air sources, air flow control valves, a set of the heat exchanger, and measurement devices. The DSC blocks are made of hydrophilic polymer-based sorbent. The structure of DSC blocks is arranged as a honeycomb structure with a square shape with 20 cm x 20 cm x 20 cm dimensions, as shown in Fig. 2. Eight DSC blocks are employed as the test section and arranged as two columns and two rows.

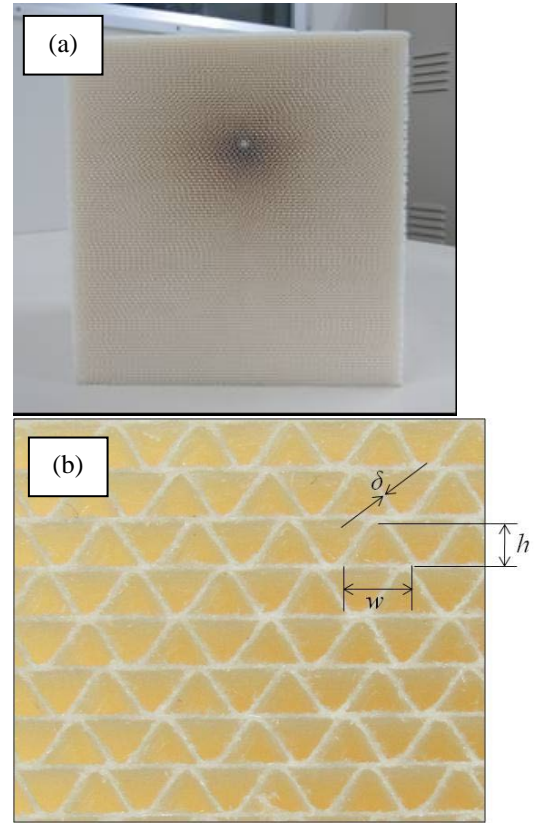


**Figure 2.** The honeycomb structure of the DSC  
(a) DSC block material,  
(b) magnification of honeycomb structure.

Two alternate operation modes that consist of dehumidification and regeneration are controlled to ensure the continuous running of DDS. At the beginning of the process, the DSC block is regenerated to remove the moisture content in the DSC material. In regeneration process, hot air is supplied by the air circulator APSITE: PAU-H3200-6KHC. The air circulator is equipped with the temperature and relative humidity (RH) controllers within an accuracy of  $T_{ac} = \pm 0.5^\circ\text{C}$  and  $RH_{ac} = \pm 2\%$ . This circulator could provide the temperature and RH in the range of 0-55°C and 0-85%, respectively. However, a set of the heat exchanger is connected to the regeneration airside for supplying high temperature of the regeneration air. In this study, the regeneration air temperature ( $T_{reg}$ ) and relative humidity ( $RH_{reg}$ ) are constants in the value of  $\pm 55^\circ\text{C}$  and  $\pm 5\%$ , respectively. While the regeneration air is flowing through the DSC block, the heat and moisture are taken by the process air. As a result, the DSC turns out to be dry which recovers the dehumidification capacity. For dehumidification mode, the process air is provided by the air circulator PAU-AZ1800SE within an accuracy of  $T_{ac} = \pm 0.05-0.1^\circ\text{C}$ . The process air temperature ( $T_{pa}$ ) is varied in the value of 20°C, 25°C, and 35°C. Mass flow rate of dehumidification and regeneration is considered as a constant parameter of 0.1 kg/s. During the dehumidification process, the DSC adsorbs the moisture

from the process air. Then the hot air is discharged to the ambient temperature. Moreover, the HMT process inside the DSC blocks is completed at the end of dehumidification period. For controlling the period of the regeneration and dehumidification processes, four different switching time ( $t_s$ ) ratios of (60 min: 60 min), (60 min: 90 min), (60 min: 120 min) and (90 min: 120 min) are also introduced in this study. The ratio of time represents the period of the regeneration compares to the corresponding dehumidification process.

## 2.2 Measurement and devices

The test apparatus is equipped with the measurement devices for temperature, RH, and flow rate. The dry bulb temperature and RH of the inlet and outlet of the DSC block are measured by the temperature and relative humidity sensor VAISALA: HMR 333 within an accuracy of  $T_{ac} = \pm 0.2-0.3^\circ\text{C}$ ;  $RH_{ac} = \pm 1-1.7\%$ . Orifice meter is employed for measuring the air flow rate. The circular orifice meter is connected to the differential pressure transmitter (TESTO: 6349) within an accuracy of  $P_{ac} = 0.35 \text{ Pa} + 0.6\%$  of full scale. For recording the data, the data acquisition unit (DAQMASTER: MX 100, accuracy =  $\pm 0.01\%$ ) is also occupied. All the data experiments are recorded automatically every 10 seconds by the data logger. When operating condition changes from the regeneration process to the dehumidification process and vice versa, the data will be stabilized after a few seconds. The experimental data will be collected for analyzing.

## 2.3 Experimental Data Analysis

The schematic diagram of the HMT process between the air and DSC wall is represented in Fig. 3.

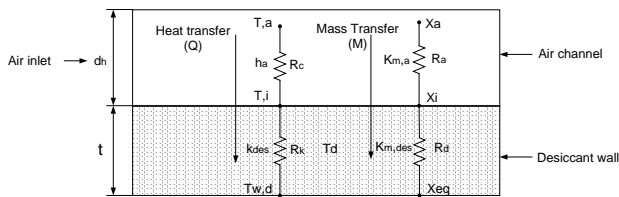


**Figure 3.** Schematic diagram of the HMT process between air and DSC wall.

During the dehumidification and regeneration process, the HMT occurs between the air and DSC material. Heat transfer ( $Q$ ) process consists of two modes; latent heat transfer ( $Q_{\text{latent}}$ ) referring the phase change of the adsorbed molecules and sensible heat transfer ( $Q_{\text{sensible}}$ ) associating with the temperature difference of the air. Also, mass transfer ( $M$ ) is composed of moisture transport and latent heat transport as the phase change of the adsorbed molecules. It is obviously depicted also the thermal and mass resistance on Fig. 3. There are two thermal resistances for the heat transfer: convection on

the air area ( $R_c$ ) and conduction in the DSC wall ( $R_k$ ). Furthermore, Fig.3 shows two mass transport resistances: resistance of the bulk air ( $R_a$ ) and resistance of the DSC side ( $R_d$ ). The thermal and mass resistance are evaluated to determine the overall HMT coefficient. Moreover, the overall HMT coefficient is used to calculate the convective heat transfer ( $h$ ) and mass transfer ( $k_t$ ) coefficient.

The mass transport rate on the DSC side ( $M_d$ ) is evaluated based on the humidity and mass transfer coefficient<sup>(11)</sup> in the following expression:

$$M_d = k_{m,des} A_a (X_i - X_{eq}) \quad (1)$$

where  $k_{m,des}$  is the mass transfer coefficient of the DSC side ( $\text{kg}(\text{m}^2\text{s}^{-1})$ ).  $A_a$  is the area of the air side ( $\text{m}^2$ ).  $X_i$  is the humidity ratio of the air-DSC interface ( $\text{kg/kg}$ ).  $X_{eq}$  is the humidity ratio of the DSC side ( $\text{kg/kg}$ ).

On the other hand, the mass transfer rate on the air side ( $M_a$ ) can be evaluated by:

$$M_a = k_{m,a} A_a (X_a - X_i) \quad (2)$$

where  $k_{m,a}$  is the mass transfer coefficient of the air side ( $\text{kg}(\text{m}^2\text{s}^{-1})$ ),  $A_a$  is the area of the air side ( $\text{m}^2$ ), and  $X_a$  is the humidity ratio of the air side ( $\text{kg/kg}$ ).

Hence, the total mass transfer ( $M$ ) is defined by:

$$M = k_{tot} A_a (X_a - X_{eq}) \quad (3)$$

Considering the mass transfer coefficient of the DSC side and air side, total mass transfer coefficient ( $k_{tot}$ ) is expressed as follows:

$$\frac{1}{k_{tot}} = \frac{1}{k_{m,des}} + \frac{1}{k_{m,a}} \quad (4)$$

The heat transfer between the air and DSC side consists of  $Q_{\text{latent}}$  and  $Q_{\text{sensible}}$ . The total heat transfer rate ( $Q$ ) is analyzed by the following equation:

$$Q = h_a A_a (T_a - T_i) + M \cdot q_{st} \quad (5)$$

where  $h_a$  is the air side heat transfer coefficient ( $\text{kW}(\text{m}^2\text{K})^{-1}$ ),  $T_a$  is the air temperature (K),  $T_i$  is the temperature of the interface between the air and DSC surface, and  $q_{st}$  is the adsorption heat ( $2500 \text{ kJkg}^{-1}$ ).

## 3. Results and Discussion

Clarifying the reliability of the system, the HMT balance under the different inlet air conditions is provided in this present work. The HMT balance is evaluated by calculating the difference between the dehumidification and regeneration process for each variation.

### 3.1 Humidity ratio and relative humidity of DDS.

The influence of the three different process air temperatures (20°C, 25°C and 35°C) on the humidity ratio ( $X$ ) and relative humidity (RH) of the inlet and outlet air of the DDS are depicted on the Figs. 4 and 5, respectively. Based on the psychrometric background, the humidity ratio and RH are closely linked with the moisture content of the air. Hence, it can be assumed that the ability of the DSC material to adsorb the moisture from the moist air is defined as a function of the partial pressure of moist air divided by the saturation pressure or RH. This saturation vapor pressure is only the function of the temperature<sup>15</sup>. In general, the regeneration air has a high temperature (80 °C - 120°C) with low RH. However, the present study is investigated in low regeneration temperature ( $T_{reg}$ ) of 55°C to allow the use of low-grade waste heat and solar energy<sup>16</sup>. This temperature is also selected with the aim to achieve the optimum dehumidification performance of the system<sup>17</sup>.

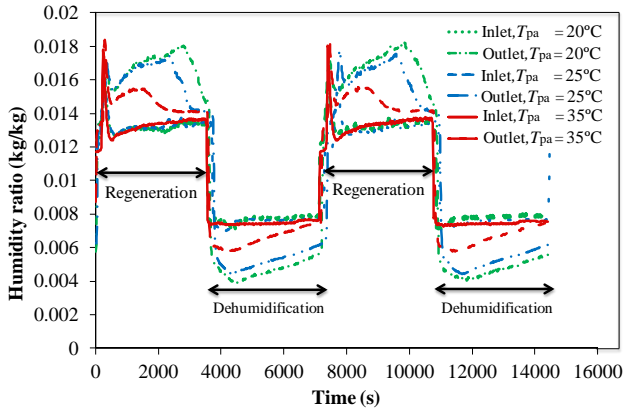


**Figure 4.** Humidity ratio ( $X$ ) of the inlet air at switching time ( $t_s$ ) of 60 min: 60 min.

In the regeneration process, the water movement takes place from the DSC material towards the airstream. Hence, the DSC moisture content decreases but the temperature and surface water vapor of the DSC increases. In the other hand, the moisture of the regeneration air stream rises while the temperature decreases. As expressed in Figs 4 and 5, during the regeneration process, the humidity ratio and RH of the outlet air are higher than those of the inlet. For all cases, humidity ratio and RH of the outlet air tend to decrease over the time and show the similar value with the outlet at the end of the process. Conversely, the humidity ratio and RH of the outlet air are lower than the inlet during the dehumidification process. The process air with higher relative humidity ratio is exposed to the dry DSC material. This process is allowed the heat of adsorption released from the DSC material, which has a high temperature, towards the airstream. During the contact with DSC material, the process air is dehumidified, and the temperature of the air is nearly constant<sup>11</sup>.

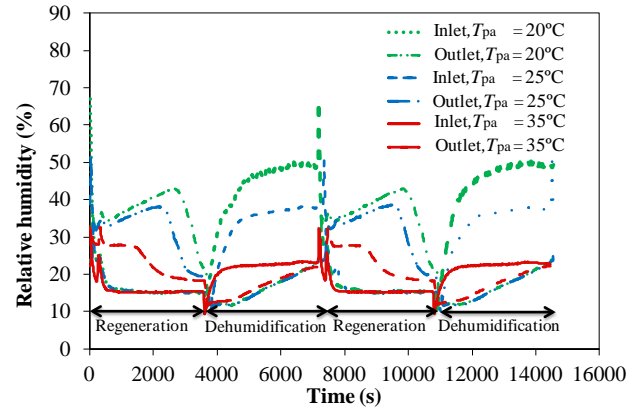


**Figure 5.** Relative humidity (RH) of the outlet air at switching time ( $t_s$ ) 60 min: 60 min.

In addition, it is also shown in Figs. 4 and 5 that the low temperature of the process air has a high potential to remove the amount of the moisture. It can be explained, when the temperature increases the RH, humidity ratio decreases. Consequently, the water content also decreases. This phenomenon indicates that the water vapor pressure increases with the increase of humidity ratio. As a result, the potency of mass transfer also increases<sup>18</sup>.

### 3.2 Dehumidification Index

Dehumidification index is defined as the differences between the humidity ratio inlet and outlet of the air during the dehumidification and regeneration process. It shows the capability of the desiccant material to adsorb/desorb the water vapor from the air. A contour plot for dehumidification index with three different process air temperatures is plotted on Fig. 6. In general, the dehumidification and regeneration processes play an essential role in the shape contour of the cycle. Regarding Figs. 4 and 5, during the dehumidification process, the heat of adsorption is released so that the temperature of the air increases and its humidity decreases. Thus, the vapor difference as a driving force for dehumidification reduces. Moreover, the dehumidification ability is also limited<sup>19</sup>. It also can be observed from Fig. 6 that the different process air temperatures give different potential dehumidification capacity.



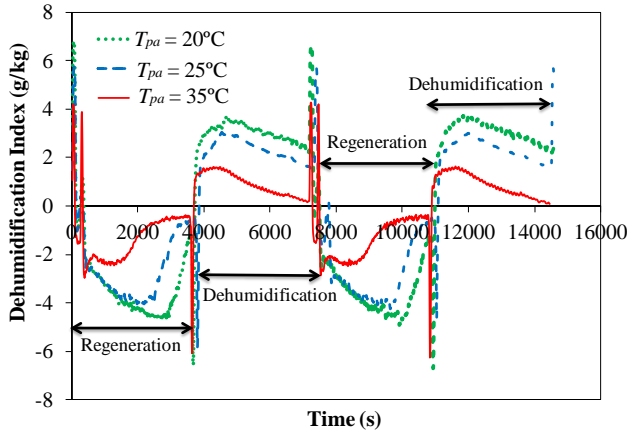


**Figure 6.** Dehumidification index at switching time of 60 min: 60 min.

The increase of the dehumidification capacity is due to the improvement of the convective mass transport between the air and the DSC. The dehumidification indexes for each variation ( $T_{pa} = 20^\circ\text{C}$ ,  $25^\circ\text{C}$  and  $35^\circ\text{C}$ ) are found in the values of 4.7 g/kg, 2.7 g/kg, and 0.5 g/kg, respectively.

### 3.3 Heat and mass balance

The effect of the process air temperature ( $T_{pa}$ ) and switching time ( $t_s$ ) on HMT characteristics was evaluated by using the Eqs. (1) – (5). However, due to the complexities to measure the properties of interface between the air and DSC wall, Eqs. (1) – (3) were simplified. Total mass transfer rate was calculated by:

$$M = \dot{m}_a |X_{a,in} - X_{a,out}| \quad (6)$$

where  $\dot{m}_a$  was the mass flow rate of the process air during dehumidification and regeneration,  $X_{a,in}$  and  $X_{a,out}$  were the humidity inlet and outlet of the air. While for the heat transfer rate in Eq. (5), sensible heat ( $Q_{sensible}$ ) was calculated by:

$$Q_{sensible} = \dot{m}_a (T_{a,in} - T_{a,out}) \quad (7)$$

where  $T_{a,in}$  and  $T_{a,out}$  were the temperature inlet and outlet of the air. The mass flow rate and face velocity of the process air during the dehumidification and regeneration were constant in the value of 0.1 kg/s and 0.094 m/s, respectively. From the Eqs. (1) - (7), it shows that the HMT was mainly affected by the changing of temperature and humidity ratio of the air.

The plotting of mass transfer rate with time for dehumidification and regeneration process for the process air temperature of  $20^\circ\text{C}$  and switching time ( $t_s$ ) ratio of 60 min: 60 min is shown in Fig. 7. It can be observed that the mass transfer rate of the regeneration process generally is higher than the dehumidification process.

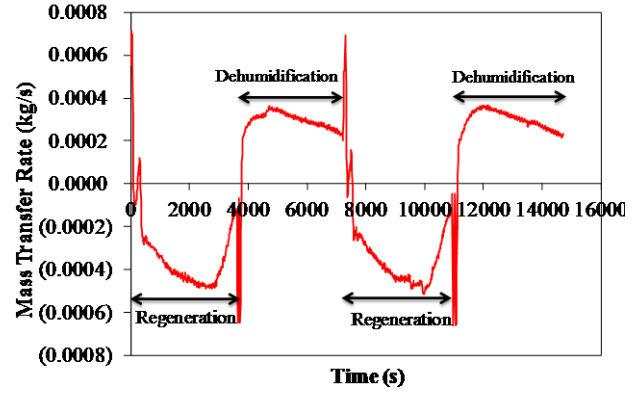


**Figure 7.** The variation of mass transfer rate with time at process air temperature of  $20^\circ\text{C}$  and switching time of 60 min: 60 min.

The mass transfer of the regeneration and dehumidification process mainly depends on the humidity ratio of the process. Since the difference of the humidity ratio of the regeneration process is higher than that of the dehumidification process, the mass transfer of the regeneration process is also higher than dehumidification process. Furthermore, the hot and dry air at the regeneration process has a higher air vapor pressure consequently the mass transfer is also higher than the dehumidification process. The differences between both processes decrease with the increase of the time. However, for cyclic operation the mass adsorbed must be the same as that of regenerated<sup>20</sup>. Hence, a proper selecting period (switching time) for each operation becomes crucial.

The mass transfer balance for the different inlet air temperatures is represented in the Fig. 8. For all cases, the mass balance offers the similar tendency.

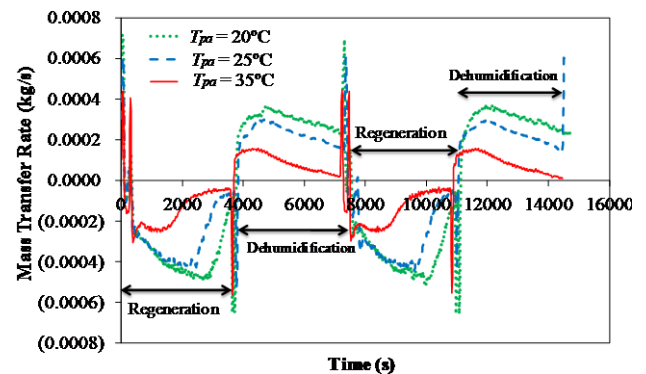


**Figure 8.** The mass transfer rate for three different inlet air temperatures at switching time 60 min: 60 min.

As shown in Fig 8, the increase of process air temperature will decrease the mass transfer rate of desiccant dehumidification system. The air-vapor pressure and adsorption potency will decrease when the inlet air temperature rises. It can also be justified from Fig. 4 that the increase of inlet air temperature will decrease the humidity ratio which is considerably

affected the reduction of the moisture removal capacity. Based on the Eq. 3, the mass transfer of the DDS is determined by the humidity ratio which is positively correlated with the moisture removal capacity. However, the humidity gradient in the air stream that has adsorbed/desorbed makes an important role to drive the migration of the water molecule. In other words, the mass transport occurs due to the difference in mass concentration<sup>21)</sup>. In the dehumidification process, the surface of the desiccant material has higher water concentration than the center. It causes the water to diffuse inward. Additionally, as the mass flow rate and face velocity were constant, the dehumidification process was longer than regeneration process.

Figure 9. shows that  $Q_{total}$ ,  $Q_{sensible}$  and  $Q_{latent}$  at process air temperature and switching time for 20°C and (60 min: 60 min), respectively. In the regeneration process, the DSC material has lower humidity and temperature than the airstream. Hence, the heat is transferred from the hot air to the DSC material. The total heat transfer rate for regeneration process can be defined as the differences between the  $Q_{sensible}$  and  $Q_{latent}$ . Thus, in the regeneration process, the  $Q_{total}$  can be lowered than  $Q_{sensible}$ . Whereas, in the dehumidification process, when the humid air meets the DSC material the heat is transferred from the DSC material to the air stream.  $Q_{total}$  for the dehumidification process is calculated by summing the  $Q_{latent}$  and  $Q_{sensible}$ . From Fig. 9, the  $Q_{total}$  for both processes offers the same trend. The  $Q_{total}$  tends to decrease with the increase of time because of the decrease in mass transfer<sup>11)</sup>. Further, the effect of the temperature difference is more prominent than the phase change of the adsorbed moisture. It can be shown from the Fig.9 that the  $Q_{sensible}$  is higher than  $Q_{latent}$ . The similar trend appears for all cases.

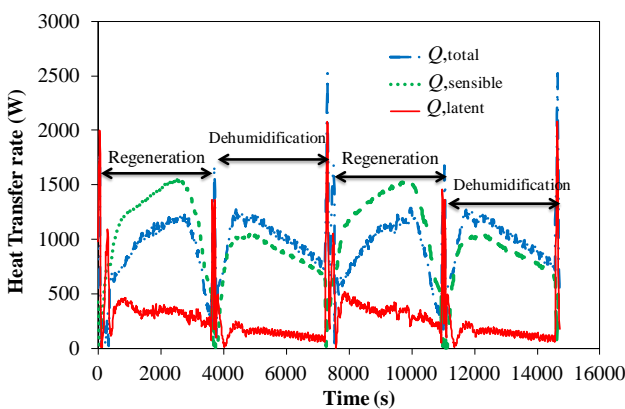


**Figure 9.** The variation of heat transfer rate with time at process air temperature and switching time for 20°C and (60 min: 60 min), respectively.

Also, the HMT balance is calculated to clarify the reliability and feasibility the present experimental data. Based on the thermodynamic principle, the HMT of the dehumidification and regeneration processes must be

balanced. In this work, the difference between the HMT of the dehumidification and regeneration process is found less than 8%. The details of HMT for all cases are resumed in Tables 1 and 2.

**Table 1.** The discrepancy of the heat transfer of the DDS for all cases.

$t_s$ (min:min)	60:60	60:90	60:120	90:120
$T_{pa}$ (°C)				
20	7.1%	4.3%	7%	4.4%
25	5.7%	4.4%	4.4%	5.6%
35	4.7%	4.5%	3.7%	7%

**Table 2.** The discrepancy of the mass transfer of the DDS system for all cases.

$t_s$ (min:min)	60:60	60:90	60:120	90:120
$T_{pa}$ (°C)				
20	1.04%	2%	2.5%	5.3%
25	1%	2.8%	4.4%	2.2%
35	1.8%	3.6%	6%	4.5%

Additionally, all the data (Figs. 4-9) shows overshoot at the time between the dehumidification and regeneration. Alternating the process between regeneration and dehumidification was completed by switching the air flow control valves. Due to a sudden change of the pressure and temperature of the air, thus all data is overshoot.

#### 4. Conclusions

The experimental study of the DDS under three different air inlet temperatures and four different switching times has been done. The concluding remarks can be drawn as follows:

- At higher humidity ratio, the DSC will get higher moisture removal.
- Moisture removal mass increases with increasing RH, in due to the higher mass transfer potential between air and DSC.
- The dehumidification capacity of the DSC system shows that the DDS has a high potential as air conditioning devices.
- The heat and mass balance are shown the discrepancy less than 8%, those of the experimental methods are reliable to conduct a further experiment.

#### Acknowledgment

The author wishes to thank the Ministry of Research,



Technology, and Higher Education and Ministry of Finance, the Republic of Indonesia for the scholarship within the framework of BUDI-LN.

### References

- 1) P. Majumdar, W.M. Worek, *Heat Recovery Syst. CHP*, **9**, 299-311 (1989).
- 2) P.L. Dhar, S.K. Singh, *Appl. Therm. Eng.*, **21**, 119-134 (2001).
- 3) Q. Cui, H. Chen, G. Tao, H. Yao, *Energy*, **30**, 273-279 (2005).
- 4) F. E. Nia, D. Paassen, M.H. Saidi, *Energy Build.*, **38**, 1230-1239 (2006).
- 5) P. Stabat, D. Marchio, *Appl Energy*, **85**, 128-142 (2008).
- 6) R. Wang, L. Wang, J. Wu, *Adsorption Refrigeration Technology Theory and Application*, John Wiley and Sons, Singapore (2014).
- 7) P. Majumdar, *Sol Energy*, **62**, 1-10 (1998).
- 8) L.A. Sphaier, W.M. Worek, *Int J Heat Mass Transf*, **47**, 3415-3430 (2004).
- 9) H. Inaba, F. Komatsu, A. Horibe, N. Haruki, A. Machida, *Heat Mass Transf*, **44**, 1305-1313 (2008).
- 10) C.E.L. Nobrega, N.C.L. Brum, *Energy Build.*, **50**, 251-258 (2012).
- 11) Z. Li, S. Michiyuki, F. Takhesi, *Int J Heat Mass Transf*, **89**, 641-651 (2015).
- 12) H. Kang, D. Lee, *Energy*, **120**, 705-717 (2017).
- 13) C. Chang, W. Luo, C. Lu, Y. Cheng, B. Tsai, Z. Lin, *Science, and Technology for the Built Environment*, **23**, 81-90, (2017).
- 14) M. Sultan, T. Miyazaki, S. Koyama, Z. M. Khan, *Adsorpt. Scie. and Technol.*, **0(0)**, 1-16 (2017).
- 15) ASHRAE Handbook, *Fundamentals*, Psychrometrics Chapter 1, p. 1.8-1.9 (2013).
- 16) M. Sultan, I.I. El-Sharkawy, T. Miyazaki, B.B. Saha, S. Koyama, *Evergreen*, **01**, 5-11 (2014).
- 17) M. H. Mahmood, M. Sultan, T. Miyazaki, S. Koyama, *Proc. 16<sup>th</sup> Int. Refrigeration and Air Conditioning Conference*, 2261, 1-10, USA (2016).
- 18) C.G. Moon, P.K. Bansal, S. Jain, *Int. J. Refrig*, **32**, 524-533 (2009).
- 19) D. La, Y.J. Dai, Y. Li, R.Z. Wang, T.S. Ge, *Renew Sustainable Energy Rev.*, **14**, 130-147 (2010).
- 20) A.M. Hamed, *Renew. Energy*, **28**, 2099-2111 (2003).
- 21) R. B. Bird, W.E. Stewart, E.N. Lightfoot, *Transport Phenomena*, John Wiley & Sons, Inc, London (1960).